



Segmentation methods of H&E-stained histological images of lymphoma: A review



Thaína A. Azevedo Tosta^{a,b,*}, Leandro A. Neves^c, Marcelo Z. do Nascimento^{a,b}

^a Faculty of Computer Science (FACOM) - Federal University of Uberlândia (UFU), Av. João Naves de Avila, 2121, 38400-902, Uberlândia, MG, Brazil

^b Center of Mathematics, Computing and Cognition (CMCC), Federal University of ABC (UFABC), Av. dos Estados, 5001, 09210-580, Santo André, SP, Brazil

^c Department of Computer Science and Statistics (DCCE), São Paulo State University (UNESP), R. Cristóvão Colombo, 2265, 15054-000, São José do Rio Preto, SP, Brazil

ARTICLE INFO

Keywords:

Segmentation
Chronic lymphocytic leukemia
Follicular lymphoma
Mantle cell lymphoma
Histological images

ABSTRACT

Image processing techniques are being widely developed for helping specialists in analysis of histological images obtained from biopsies for diagnoses and prognoses determination. Several types of cancer can be diagnosed using segmentation methods that are capable to identify specific neoplastic regions. The use of these computational methods makes the analysis of experts more objective and less time-consuming. Thus, the progressive development of histological images segmentation is an important step for modern medicine. This study presents the progress of recent advances in methods for segmentation of chronic lymphocytic leukemia, follicular lymphoma and mantle cell lymphoma images. The paper shows the main techniques of image processing employed in the stages of preprocessing, detection/segmentation and post-processing of published approaches and discusses their advantages and disadvantages. This study presents the most often used segmentation techniques for these images segmentation, such as thresholding, region-based methods and K-means clustering algorithm. The addressed cancers are also described in histological details as well as possible variations in the tissue preparation and its digitization. Besides, it includes a review of validation techniques and discusses the potential future directions of research in the segmentation of these neoplasias.

1. Introduction

Cancer incidence throughout the world has become ever more relevant due to its epidemiological profile. In 2030, 21.4 million new cases and 13.2 million deaths due to cancer are estimated [1]. Lymphoma is a type of cancer affecting the lymphatic system classified into at least 38 subtypes [2]. These subtypes are divided into Hodgkin lymphomas (HL) and non-Hodgkin lymphomas (NHL) in accordance with their morphological, immunophenotypical, genetical and clinical features [3]. Global records of 2012 show that 199 thousand NHL-related deaths and 254 deaths resulting from HL occurred during that year [1].

This paper addresses published studies of chronic lymphocytic leukemia (CLL), follicular lymphoma (FL) and mantle cell lymphoma (MCL), which are part of the NHL class. This class corresponds to 70% of lymphomas cases and due to its wide range of clinical presentations and histopathological features, its classification and segmentation still represent a major challenge for pathologists [4]. CLL represents a different manifestation type of small lymphocytic lymphoma, so both of these are dealt with in the same manner. FL is the second most common

type of Bcells lymphoma. Concerning MCL, it is characterized by an aggressive clinical evolution with few survivors in the long term [5].

To diagnose NHL, a specialist analyses tissue samples stained with, for example, hematoxylin-eosin (H&E) to identify cancerous regions. These distinctions are essential for disease monitoring, identification of its stage and orientation towards appropriate treatments for the patient [2]. However, visual evaluation is a complex task due to experience level, subjective analysis and inter-pathologists variability [6]. For a more objective process, histological samples digitization has enabled significant advances in the research of diagnoses and prognoses using computational techniques, called computer-aided diagnosis (CAD). These systems have the potential to aid pathologists in their clinical decisions associating image information with diseases features [2,7,8].

CAD systems can also be applied to radiological images. Since these images are different from the histological ones, different image processing techniques are required [9]. Due to their less amount of objects of interest, that are limited to specific organs of the body, and their gray-scale intensities, the histological images allow more processing than these images [10]. Besides, the identification of cancer subtypes is

* Corresponding author. Center of Mathematics, Computing and Cognition (CMCC), Federal University of ABC (UFABC), Av. dos Estados, 5001, 09210-580, St. André, SP, Brazil.
E-mail addresses: tosta.thaina@gmail.com (T.A. Azevedo Tosta), neves.leandro@gmail.com (L.A. Neves), marcelo.zanchetta@gmail.com (M.Z. do Nascimento).

practically impossible on radiological images [9].

One of the major challenges for histopathological image analysis is the segmentation, that is capable to recognize important regions for diagnoses, such as nuclei and glandular structures, and their features [11]. Accurate identification of regions of interest (ROIs) is essential to correlate them to pathologies [12]. The large variability in histological features of different lymphomas leads to the development of algorithms that could contribute to improving image analysis procedures and/or CAD systems related to CLL, FL and MCL.

Given the recent advances of CAD systems, this review describes and discusses different methods suggested in the literature for segmentation of CLL, FL and MCL histological images. The main emphasis of investigating segmentation of histological images is due to some issues involved for this purpose. For instance, there is a wide variation in the image quality (tissue preparation), digital acquisitions (artifacts introduced by the compression of the image and/or presence of digital noise) and nuclei overlapping [17,18]. This study identifies the most often methods of lymphoma images segmentation, such as thresholding, region-based methods and K-means clustering algorithm. The major contribution of this study is found in the discussion of the main processing techniques of lymphoma histological images, therefore, providing directions for future research.

This paper is organized into six sections. Section 2 presents definitions and details about lymphoma and its different subtypes considered

in this study. Cellular features of CLL, FL and MCL are also described in that section as an insight for development of processing techniques of these images. In section 3, the stages of tissue preparation and their possible variations are presented for histological images acquisition. Sections 4 and 5 introduce theoretical concepts required for a better understanding of techniques for CLL, FL and MCL analyses. Discussion and future directions for research of lymphoma images segmentation considering limitations from published articles are presented in Section 6.

2. Lymphoma

Lymphoma is a disease developed in cellular structures responsible for immunological defense of the body, called lymphocytes [2,19]. Originating from bone marrow, lymphocytes are subdivided into B lymphocytes, T lymphocytes and null cells [20]. These diseases may develop in B cells as well as in T cells, however, 85% of cases are derived from B lymphocytes [2]. Development, activation and differentiation of normal B cells can be divided into three stages: pre-germinal center, germinal center and post-germinal center. Fig. 1 represents these B cell development stages and a few lymphomas related to each one of them [21].

Lymphomas cases originate in lymph nodes of lymphatic system, with higher frequency located in the neck, armpits, groin and along large

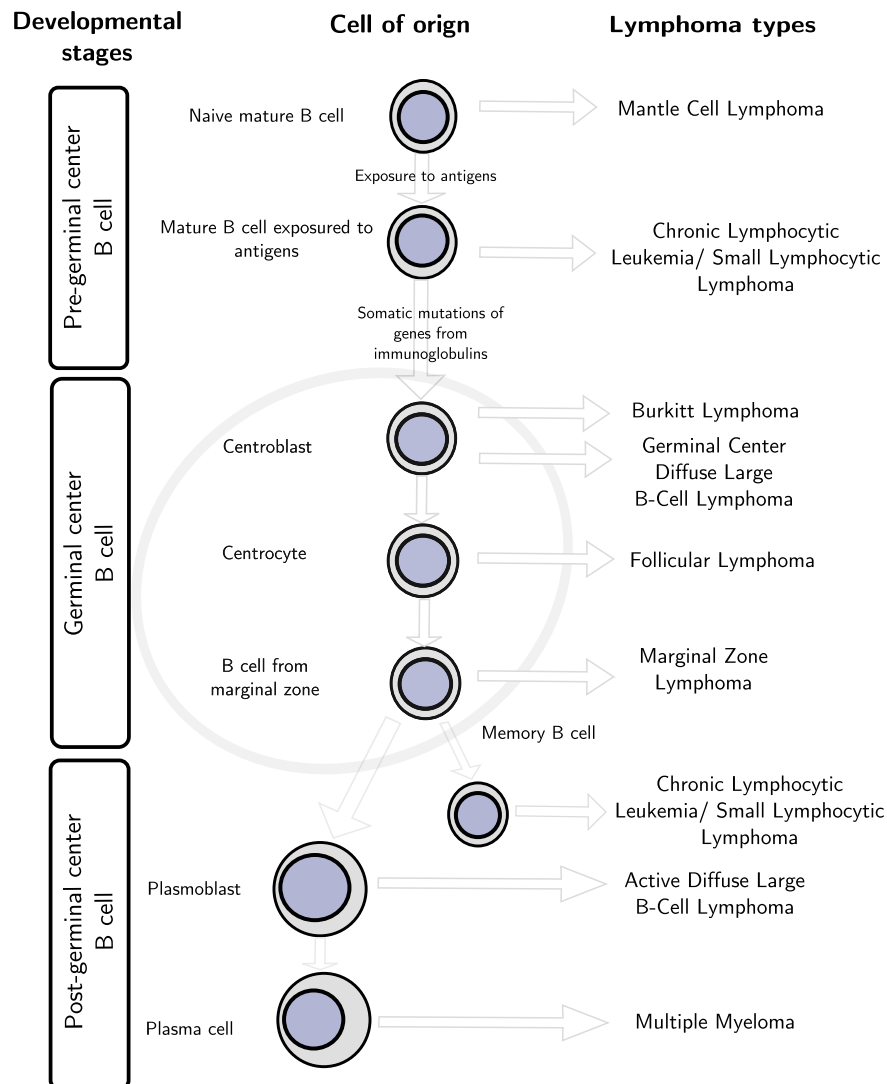


Fig. 1. Stages of development, activation and differentiation of B cells related to different lymphomas. Figure extracted from [21] (© 2012).

blood vessels. These organs act as filters to remove bacteria and other unfamiliar substances that reach them [19,20]. Different types of lymphoma are usually distinguished by their growth patterns and their cytological features, such as the morphological ones that can be used in image processing to identify cells that will allow the classification of the disease [22,23].

2.1. Chronic lymphocytic leukemia

CLL is considered lymphoproliferative due to lymphoid cells proliferation. These cells are in their maturing stage but they are immunologically incompetent [5,24]. In most cases, it is characterized by small lymphocytes with regular nuclei and condensed chromatin, without evident nucleoli and scant cytoplasm. Furthermore, the number of prolymphocytes, characterized by their medium size with abundant cytoplasm and evident nucleoli, is less than 10% [24]. CLL may present some similarities with MCL, however these cases can be distinguished by cellular features. Small lymphocytes with condensed chromatin are predominant, with variations in their nuclear morphologies [5].

The CLL diagnosis usually begins with lymphocytes counting, that must correspond to at least $5 \cdot 10^9$ B lymphocytes/L of peripheral blood. The identification of CLL cells in blood is based on the search for small and mature lymphocytes, with a thin border of cytoplasm and a dense nucleus with undistinguished nucleoli. Lymph node biopsy is required for confirmation of an evolution to an aggressive lymphoma [25]. Fig. 2 displays a CLL tissue sample stained with H&E [26].

2.2. Follicular lymphoma

FL is characterized by a cell group with partial follicular growth pattern covering lymph nodes cavities, called follicular centers [5]. Some cellular types present in normal follicular centers can also be observed in these pathological regions. They are the centrocytes characterized by their small size, cleaved nuclei, scarcely discernible nucleolus and pale cytoplasm, and the centroblasts corresponding to large cells, with round or oval shape and nuclei with 1 or even 3 nucleoli. Neoplastic follicles are poorly defined and present low concentration of B lymphocytes [3]. Fig. 3 shows a H&E-stained FL image [26].

FL diagnosis is based on lymph node biopsies and must be obtained according to the World Health Organization classification considering the centroblasts absolute number in the neoplastic follicle [3,27]:

- Grade I: between 0 and 5 centroblasts;
- Grade II: between 6 and 15 centroblasts;
- Grade III: more than 15 centroblasts.

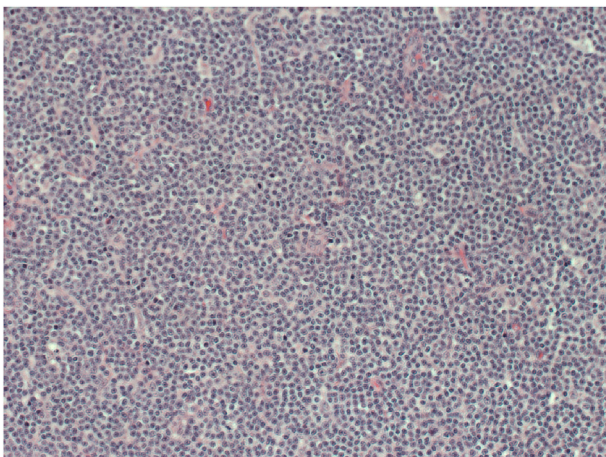


Fig. 2. CLL tissue sample with 20× magnification and 1388 × 1040 pixels. Figure extracted from the public dataset of [26] (© 2008 Springer).

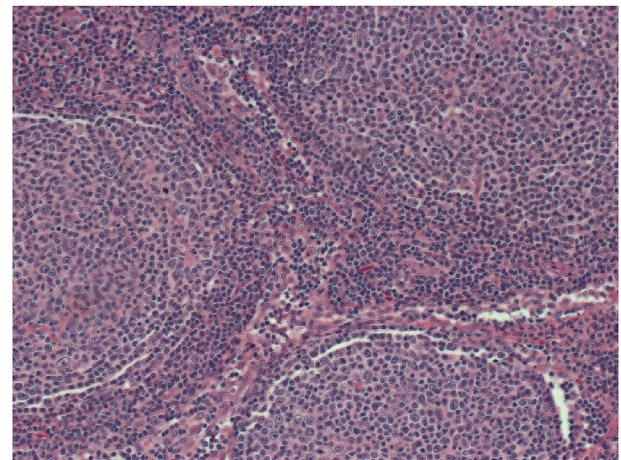


Fig. 3. FL histological image with 20× magnification and 1388 × 1040 pixels. Figure extracted from the public dataset of [26] (© 2008 Springer).

In new classification, grade III may also be divided into III-A when centrocytes are present and III-B when centroblasts form groupings. The III-B grade is considered an aggressive lymphoma and must be treated as such. Grades I, II and III-A must be treated as indolent. It is advisable that tissue samples of III-A and III-B grades be reviewed by specialists if the infiltration pattern is atypical (diffuse areas with small cells) [27].

2.3. Mantle cell lymphoma

MCL is characterized by cleaved cells with small/medium size with a vaguely nodular and diffuse proliferation, or mantle zone enlargement, which is a concentrated region of B lymphocytes surrounding germinal centers [19]. Furthermore, these cells usually have comparable sizes and share similar cytological features: size slightly larger than normal lymphocytes with condensed chromatin, a small amount of cytoplasm, imperceptible nucleoli and a cleaved irregular nuclear contour. Cells similar to centroblasts are absent, providing an important distinction between this disease and the FL [3,5].

MCL is diagnosed through the identification of tumors with a morphological analysis of irregular cell nuclei with small/medium size. However, MCL lymphocytes can be presented by variant morphologies, such as small round cells and marginal zone-like lymphocytes. A minority of these cases are correctly identified, which makes advisable the review by a pathologist [28]. Fig. 4 presents a slide of MCL tissue sample stained with H&E [26].

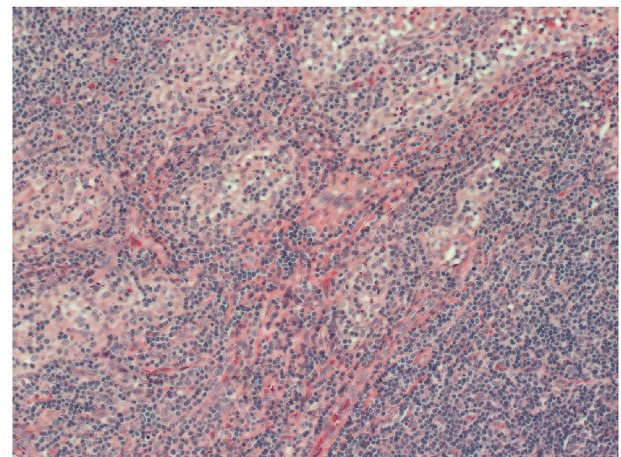


Fig. 4. A MCL tissue sample digitized with 20× magnification and 1388 × 1040 pixels. Figure extracted from the public dataset of [26] (© 2008 Springer).

3. Tissue preparation

Histology is responsible for tissues study and how they are organized in forming organs [19,20]. However, histology also forms a direct relationship with other areas, such as the pathology [19].

Different techniques were developed for preparing tissue samples allowing for their analyses [19]. Tissue preparation steps involve the manipulation of a small tissue sample obtained from biopsy, or other techniques. These tissues must be removed in a carefully monitored way so that there will be no distortion in their microscopic appearance. In order to achieve this, they should pass through the procedures of fixation, dehydration and diaphanization, inclusion, microtomy, mounting and staining [19,29].

In the microtomy step, the tissue block is sliced in a progressive way with a defined and identical thickness. This factor can affect histological image analysis. Tissue samples with 4–5 μm thickness allow the identification of important cell features, such as its size, shape and cytoplasm. However, lower thickness levels are able to represent nucleoli areas, which are regions analyzed in some cells classification tasks [36]. Fig. 5 illustrates FL images with 4 μm and 1 μm thickness, where it is noticeable the clear visualization of internal cell structures in the second image [30].

Stains commonly used in histology are the H&E [19,20]. Hematoxylin stains acid structures in blue-purple shades, such as nuclei [20]. On the other hand, eosin stains basic components in pink shades. Several cytoplasm areas are stained in pink from eosin since many of their components have basic pH [19]. These properties can be useful for application of segmentation methods using only intensity features.

After the tissue staining with H&E, the histological slides digitization is possible by means of digital scanners or microscopes equipped with cameras [31–33]. This technique can replace physical slides for educational purposes, remote consultancies and, mainly, for the development of images-based systems [34]. The use of computational algorithms becomes important for aiding specialists in making diagnoses and prognoses decisions [31]. Additionally, computational approaches enable faster results through the use of image processing techniques [32].

With the introduction of whole-slide scanners, CAD systems became popular, even for processing of whole-slides lymphoma images (WSI). Among the correlated studies, only five of them ([7,22,35–37]) are dedicated to WSI processing. These images were used for identification of follicular regions, typical of FL images, and for FL grading. Their use to segment cellular structures, such as centroblasts [36] or nuclear and cytoplasm regions [22], is extremely scarce. However, for segmentation of follicular regions, WSI images can be more relevant since they allow a better visualization of these structures (see Fig. 6).

One factor of histological image digitization is its magnification. Magnification allows to define the image enlargement degree [38]. This factor can influence histological image analysis since higher the magnification, more details can be visualized and used by computational

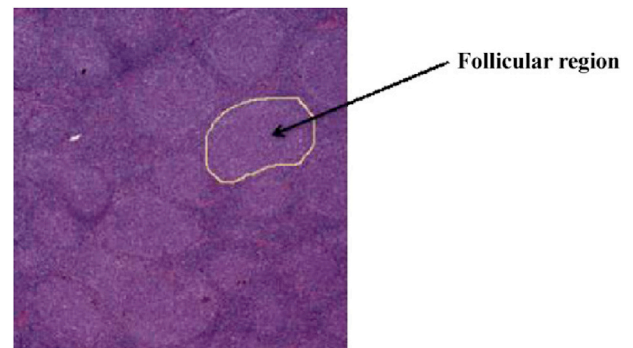


Fig. 6. An indicated follicular region in a part of a WSI. Figure extracted from [7] (2011 Elsevier).

algorithms [9]. Fig. 7 presents a histopathological tissue sample of prostate at successive incremental magnifications [39], where more cellular details can be seen at the right image.

For robustness evaluation, the IICBU Biological Image Repository database is employed as a benchmark to evaluate the image analysis algorithms for CLL, FL and MCL cases, which is available for download at [26]. A total of 30 histological slides of lymph nodes stained with H&E were obtained. To better represent clinical environments, these slides were obtained with significant variations in sectioning and staining, which, as mentioned above, can represent challenges for image processing methods [26]. For this dataset, the microscopic images were digitally obtained using a light microscope (Zeiss Axioscope) with 20 \times objective, a color digital camera (AXio Cam MR5), resolution of 1388 \times 1040 pixels and quantization of 24 bits. In total, 375 images were generated, containing 113, 140 and 122 images of CLL, FL and MCL, respectively.

4. Lymphoma histological image processing: techniques analysis

Computational methods are being widely developed for histological image-based applications, since they improve analyses through segmentation until diseases classification [17,40]. To use such techniques, steps for their application must be defined [41]. In this context and regarding the purpose of this work, the main steps for analysis are: pre-processing, segmentation, and post-processing.

4.1. Preprocessing

The preprocessing step is necessary to remove irrelevant tissue structures, enhance contrast and remove noises, among other refinements aimed before detection or segmentation. Fundamentally, it aims at improving the image quality for the segmentation.

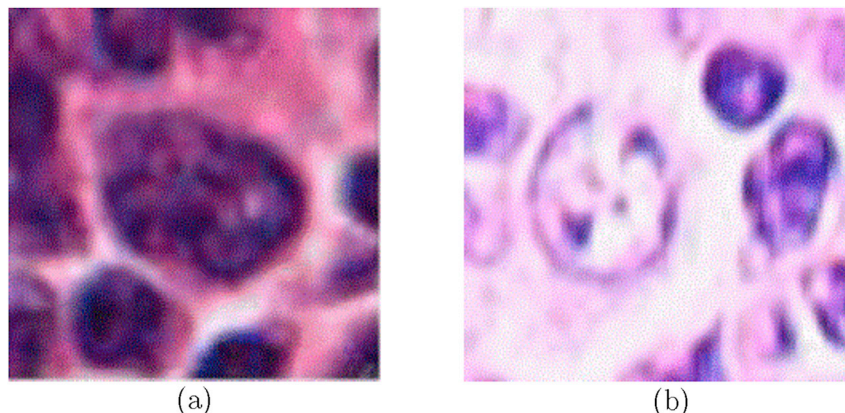


Fig. 5. FL tissue samples sliced using (a) 4 μm and (b) 1 μm thickness. Figure extracted from [30] (© 2014 IEEE).

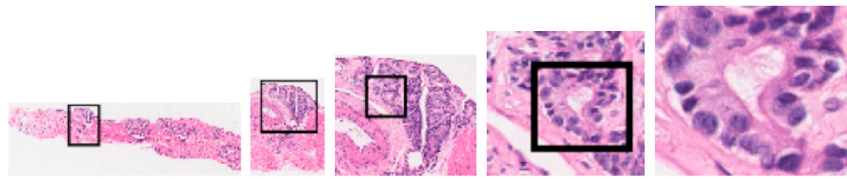


Fig. 7. Histopathological prostate image, stained with H&E, at incremental magnifications. Figure extracted from [39] (© 2006 Elsevier).

This step is commonly used by studies related to lymphoma images processing. One of the preprocessing techniques is the conversion between color models. [22,23] and [37] used the conversion from RGB model to $L^*a^*b^*$, to exploit its differences considering the application of Euclidean distance. Thus, the perceptually uniformness of $L^*a^*b^*$ allows that color changes can be compatible to visual perceptual differences [37]. Therefore, this color model can contribute to segmentation by representing colors in an independent way from illumination conditions [42]. Like the $L^*a^*b^*$ model, the $L^*u^*v^*$ color space was used by [8] and [43] due to its uniform color representation. [6] converted the RGB

images to a 1-D unitone image resulting in images with the highest contrast. To make this possible, the RGB image is projected using the principal components analysis (PCA) which associates it with the highest variance.

Another strategy that can be used in this step is channels separation. In [35], the L channel from $L^*a^*b^*$ color model was used for further processing for presenting a better contrast. The study of [44] investigated the R channel from RGB model for the same reason. Considering follicles detection on H&E images, [45] used the R and B channels from RGB immunohistochemistry-stained images (IHC) to aid in this purpose, since

Table 1
State of the art of studies related to segmentation of histological images stained with H&E of CLL, FL and MCL.

Publication year	Ref. Dataset	Objects of interest	Segmentation	Evaluation results
2006	[49] Blood images of MCL, Hairy Cell Leukemia and Plasma Cell Leukemia.	Neoplastic cells	Otsu and watershed.	There was no performance evaluation of the segmentation step.
2007	[44] The system was trained on 3627 objects and tested on 1813 FL objects.	Follicular regions	Thresholding using mean brightness value.	Maximum accuracy of 86.65%.
2008	[23] 17 whole-slide images of FL.	Centrocytes and centroblasts.	Thresholding for elimination of red blood cells and background regions in RGB color space and K-means applied on $L^*a^*b^*$ model.	There was no performance evaluation of the segmentation step.
2008	[36] 30 images of FL stained with IHC and 11 H&E-stained FL images.	Centroblasts and follicular regions.	For detection of follicular regions, co-occurrence matrix and S channel from HSV color model were used in K-means application. For centroblasts detection, features extracted were reduced by PCA and application of K-means.	Detection of follicles with sensitivity of $85.5\% \pm 9.8\%$ and specificity of $92.5 \pm 4.0\%$. Detection of centroblasts with sensitivity of 92.68% and specificity of 90.57%.
2008	[43] 18 cases of MCL, 20 of CLL, 9 of FL and 54 cases of other lymphoma types resulting in 3898 cell images.	Overlapping pathological cells.	Algorithms L_2E and gradient vector flow to estimate contours, detection of high curvature points, application of canny edge detector to model inner edges and concave vertex graph.	Accuracy of 90.1%.
2009	[37] 17 whole-slide images of FL.	Centroblasts	Thresholding and K-means.	There was no performance evaluation of the segmentation step.
2010	[6] 100 ROI of FL images.	Centroblasts	Gaussian Mixture Modeling with parameters estimation using expectation maximization.	Accuracy of 80.7%.
2010	[8] 100 ROI of FL images.	Centroblasts	Mean-shift with elimination of clusters with data points corresponding to less than 2% of the total number of these points.	Accuracy of 89%.
2010	[35] 40 FL images.	Follicular regions	Active contour model.	0.71 with a standard deviation of 0.12 using metric of Zijdenbos metric.
2011	[7] 15 FL images.	Follicular regions	Region-based segmentation using curve evolution.	78.33% by Zijdenbos similarity index and standard deviation of 2.83.
2011	[50] 10 FL images.	Cellular nuclei	Thresholding, efficient local Fourier transform, K-means and K-nn.	Average accuracy of 0.769.
2011	[51] 10 FL images.	Cellular nuclei	Thresholding, efficient local Fourier transform, K-means and K-nn.	Accuracy of cells correctly separated of 94.74%.
2012	[22] 17 FL images.	Centroblasts	K-means	There was no performance evaluation of the segmentation step.
2012	[45] 12 FL images stained with H&E and IHC.	Follicular regions	Otsu and intersection between R and B binary masks.	Indices of sensitivity, specificity, conformity and Jaccard's with maximum average of 0.935, 0.843, 0.198 and 0.57, respectively.
2013	[52] 110 FL images.	Follicular regions	Active contour model.	There was no performance evaluation of the segmentation step.
2013	[53] 132 blood cell images.	Lymphocytes	Otsu, canny edge detector and subtraction between cellular and nuclear segmentations.	Accuracies of 99.92%, 99.85% and 99.63% in nuclear, cellular and cytoplasmatic segmentation, respectively.
2013	[54] 140 blood cell images.	Lymphocytes	Otsu, K-means, support vector machine and subtraction between cellular and nuclear segmentations.	Maximum accuracies of 98.43%, 98.69% and 99.85% in nuclear, cellular and cytoplasmatic segmentation, respectively.
2014	[46] 12 images of FL.	Centroblasts	Thresholding with value of 0.37 for red blood cells removal and Otsu to segment nuclei.	Accuracy of 82.58%.
2014	[55] 300 cells contained in FL images.	Centroblasts	Thresholding and Otsu.	Detection accuracy of 90.35%.
2016	[56] 28 pairs of PAX5 and H&E stained images of FL.	Centroblasts	K-means and graph cut.	There was no performance evaluation of the segmentation step.

interfollicular regions are better represented with a lighter blue area in the IHC stain. [7] used the metrics of signal to noise ratio and texture contrast to find the channel with the best representation of follicular regions, leading to the use of B channel from the RGB model.

Other refinements were used by some articles of lymphoma image processing. In [35], the matching filter was applied to remove noises, flatten the background and enhance ROIs contours. To remove noises and small details, the Gaussian filter was applied by [46]. Besides, the histogram equalization was used in this work to enhance differences between nuclear membrane and background. Initially, [7] applied the decorrelation stretching technique to reduce the correlation between RGB channels and enhance image contrast. After selecting the B channel for further processing, the median filter was chosen to reduce noises, and the adaptive histogram equalization method was used to correct non-uniform illumination of follicles. [45] also used decorrelation stretching, median filter and adaptive histogram equalization in its pre-processing step.

4.2. Segmentation

The segmentation process is used for selecting objects of interest leading to an accurate analysis of specific structures [47]. These regions can be used for detection and classification of cancers [17]. Images are segmented based on similar regions through criteria assessment of homogeneity, such as color and texture [48].

Several published articles focus on the application of segmentation techniques to lymphoma images, with a significant portion dedicated to the study of FL. However, articles were conducted on other types of lymphomas, such as CLL and MCL. Segmentation of CLL, FL and MCL images is described in this section, as is shown in Table 1 containing the segmentation methods, along with their results and the database used for their validation. An analysis of this table indicates that lymphoma images segmentation is still little explored in the literature, even with the variety of its subtypes and ROIs.

The lymphomas segmentation methods can be divided into techniques based on histogram, edge detection and classifier methods. The ROIs in lymphoma images can be divided into follicular regions, centroblasts, centrocytes, lymphocytes and neoplastic cells. However some methods proposed the segmentation of cellular nuclei which can be applied to different histological images. The description of literature studies is organized based on these regions.

For segmentation of follicular regions, methods based on regions, thresholding and K-means clustering algorithm were proposed. Considering regions-based methods, [7,35] and [52] used the technique of Chan & Vese [57]. In this application, the initial curve iteratively moves inside the follicular region until the correspondence between this curve and the object boundary is reached by the minimization of an energy function. However, this method is not adequate to segment images with great intensity heterogeneity, making the segmentation a harder task [58]. To deal with this problem, the aforementioned works used a local calculation of the energy function, separating the internal and external regions of the objects [52].

Thresholding methods aim to define threshold values through intensity levels or image transforms [59]. One of the most popular unsupervised thresholding technique is the Otsu method [60] that was used by [45] on the R and B channels from the RGB color model. These results were combined to detect follicular regions, interfollicular areas and image background. A limitation of Otsu is its assumption of an uniform illumination condition, which demands a preprocessing step [53]. For thresholding follicular regions, [44] used as its threshold value the average intensity of the R channel from the RGB color model.

To identify follicular regions by classification of pixels, [36] used the K-means clustering algorithm with the Euclidean distance considering four classes: follicles, interfollicular regions, lymphocytes and image background. However, due to variations in the color spectrum of images, unsupervised segmentation methods can make systems more robust than

the supervised approach of K-means [37].

The thresholding methods, K-means, graph-cut, mean-shift and Gaussian mixture modeling were employed to identify centroblasts. [46] and [55] presented detections of centroblasts in which the Otsu technique was used after the removal of red blood cells by an empirical thresholding with value of 0.37. Allied to an empirical thresholding, defined by 0.45, the K-means was used by [23] and [37] to identify nuclei, cytoplasm and extracellular material with the Euclidean distance. In [22], the K-means was applied to segment centroblasts in FL images with no details about the distance metric used. In the study of [36], this method was also applied considering three classes: nucleoli, cytoplasm and inter-nucleoli material, in which the first one was the ROI.

To deal with color variations for which the K-means may not be efficient, the mean-shift algorithm was used to segment centroblasts by [8]. This algorithm was used to estimate the considered classes (nucleus and cytoplasm, extracellular material, red blood cells and image background), using the density distribution of color features of each pixel. The clusters amount was contained in the interval [50, 100], due to images color variation. To remove small amount of data, clusters with less than 2% of the total points were excluded. Subsequently, clusters were merged according to similarities of color features of the $L^*u^*v^*$ color model and spatial transitions between samples from each cluster.

Among the used methods for centroblasts segmentation, [6] used the Gaussian mixture modeling method. In this application, cellular and extracellular components were modeled by this technique in combination with the expectation maximization algorithm for parameters estimation. Also for this purpose, [56] used a thresholding method associated to graph-cut on PAX5 images, that present brown and blue colors. The segmentation is then performed by the assignment of structures to each pixel by minimizing an energy function in the graph cut. For the initial assignment of each pixel, the K-means was used. The obtained results were then registered on H&E images for texture extraction from these images.

The identification of lymphocytes was proposed by [53] and [54] on CLL blood images with high magnification. [53] used the Otsu method for nuclear segmentation. To identify cells, the canny edge detector method and the morphological operations of dilation, erosion and hole-filling were applied. Finally, the cytoplasm detection of these cells was given by the pixel to pixel subtraction of the previous segmentations. [54] also used the Otsu method for nuclear segmentation of lymphocytes. The results of this segmentation composed the training set of the support vector machine (SVM) classifier that used intensity features for pixels classification of testing images. To define the training set of the cellular segmentation, a manual segmentation was used with the subsequent application of SVM. To reduce the feature set to dimension 100, the K-means was applied.

The only work that developed the identification of centrocytes was [23] by the thresholding and the K-means clustering algorithm. For classification of FL grades, morphological and texture features were extracted and given to a Bayesian classifier. It is possible to infer the relation between this classification and the identification of centrocytes, since low grade have more centrocytes than the high grade, according to the authors.

[49] presented a method for identification of neoplastic nuclei in blood images of different lymphomas, with MCL among them. In this study, the Otsu and watershed methods were used in the segmentation step. In a detection step, features were extracted from the segmented regions and classified into health and neoplastic cells by the calculation of Euclidean distances among the feature sets.

Applicable to different types of histological images, some studies proposed the identification of cellular nuclei and overlapping cells. Thus, lymphoma images were only used to evaluate these methods. [50] and [51] segmented the RGB images by an empirical thresholding for identification of image background and red blood cells. Disregarding such regions, the features extraction was performed on the presegmented images. Then, the K-means was applied so each class could be

represented by a compact feature set. To define pixels class, their features were compared to their nine nearest neighbors, which led to two or more nuclei to be identified as one object, demanding a post-processing step.

To separate overlapping cells on lymphoma images, [43] proposed an algorithm using the gradient vector flow [61] method of active contour. To define cellular borders, this method was modified to combine estimations of initial curve points and color gradient information. Subsequently, concave points were identified, by the proposal of [62], and the inner borders detection was performed by the canny edge detector method. This step was necessary so the separation of overlapping cells could be obtained using these points and borders by the Dijkstra algorithm.

4.3. Post-processing

Post-processing techniques are applied in order to achieve segmentation results similar to those obtained by the specialist, called gold-standard [16,63]. Great part of studies related to lymphoma image processing used morphological operations in this step. In addition to using other techniques, [7,35] and [36] applied the operations of closing and object removal to eliminate tissue deformations, fill holes and smooth boundaries. Integration among dilation, hole-filling and erosion techniques was used by [46] and [53]. The first study applied these methods to correct some cells that presented open perimeters, and the second one aimed to remove some artifacts. For small refinements, [45] used dilation and removal of small objects and [37] applied only the removal of small regions.

Several articles also used the watershed algorithm. [45] applied this technique to separate concave elements, [36] used it to separate tightly clustered follicle regions and [37] identified individual cells borders. [53] used the watershed to obtain a cell mask suppressing 1% of the distance transformation local minima to reduce over-segmentation effects. Recursive watershed transform was used by [7], where H-minima and watershed transforms are adaptive to each image object to avoid over-segmentation. Besides, this study also used Fourier shape descriptors to smooth segmented regions borders. [35] also used these descriptors to eliminate irregular contours.

In order to fit ellipses to connected components, model-based intermediate representation (MBIR) was used by [22] and [37]. According to these studies, this representation can capture a higher-level description of nuclei and cytoplasm. [43] used quadratic splines to smooth boundaries obtained in segmentation and [44] used a matrix transformation associated with decision trees to identify points outside and on follicle border. [6] used size and eccentricity criteria to eliminate false positive regions, in addition to texture features extracted by gray-level run length matrix.

5. Evaluation methods of lymphoma images segmentation

In order to evaluate the proposed segmentation methods, several metrics can be used [64]. This evaluation is based on comparisons between the results of computational segmentation and manual segmentation conducted by a specialist.

The most common metrics used by studies related to CLL, FL and MCL are accuracy, sensitivity and specificity, considering the concepts of true positive, true negative, false positive and false negative [45,65]. Accuracy is able to quantify the hit rate of the proposed segmentation [64]. Sensitivity quantifies how many pixels from manual segmentation were also identified by the computational method, and specificity quantifies how many pixels outside manual segmentation were also excluded by the automatic method [45].

Another metric used in studies of lymphoma images segmentation is the Zijdenbos similarity index. This metric measures the overlapping ratio between the shapes from the manual and automatic segmentations [7,35]. Conformity and Jaccard index are another used metrics. The first one is able to measure the amount of wrongly identified pixels in relation

to the correctly identified pixels. The second one is a similarity measure between the segmentations [45].

6. Discussion and future directions

In the context of lymphoma histological images, several contributions in tissue structures segmentation have been made. However, there are still challenges that can be investigated in new researches. One of these is the evaluation of deconvolution techniques in the initial stage of lymphoma images processing. None of the described works used deconvolution methods to separate the stains into channels of color models. The use of H channel can show information of nuclear regions and the E channel can represent cytoplasm features [2]. These information may be useful for the segmentation stage.

The color variation in histopathology images can be caused by inconsistent biopsy staining and nonstandard imaging. There are various studies that investigate normalization techniques [67–69] to correct image colors that can suffer variations due to different stain manufacturers, tissues storage conditions and processes of coloring and digitization of tissue samples [66]. It was noted that no study of the lymphoma segmentation algorithms investigated the color normalization in the preprocessing step. It is important to explore this method that can improve performance of subsequent image analysis algorithms.

According to [7], application of segmentation methods in a limited number of cases may not corroborate the efficiency of proposed systems. In Table 1, there are some studies that employed a small number of samples (dataset) to evaluate their segmentation algorithms. Small amount of images was also used by [7] and [51] for parameter definition of their lymphoma segmentations. This methodology limits the robust performance of parametric methods to such small number of images. In addition to the small amount of samples, the studies of [36] and [45] used images obtained with other stains (IHC) to aid in segmentation of H&E-stained FL images. [56] used the same approach through images stained with PAX5. The use of two different types of images can be considered an obstacle to practical application of these methods. Furthermore, some studies were evaluated only for the segmentation of cells located in images central regions. The algorithms proposed by [53] and [54] are examples of the methods that investigated cells located on the central regions.

Another important aspect of CADs development is the metrics used for algorithms results validation. [45] recommends using sensitivity, specificity and conformity metrics rather than Jaccard index, since this metric can not properly express the quality of segmentation compared to the manual one. In [53] and [54], the accuracy was calculated disregarding spatial overlapping between manual and automatic segmentations. The authors in [8] calculated the accuracy using centroid locations of centroblasts identified. In Table 1, it is possible to observe that the accuracy is the most employed metric to evaluate the performance of algorithms. However, in order to make fair comparisons, it is necessary to standardize the evaluation metrics, including the accuracy [9].

Different slide preparations could not be a limitation for proposed systems. This is important considering that staining, thickness and magnification of tissue samples can impact the segmentation results [7]. The studies [6] and [37] extracted texture features from images with 40× of magnification. These features are better represented in such magnification [9], hence, leading to a poor performance when applied to low magnification images. [7] and [52] indicated limitations when applied to images with low quality and low contrast. Then, these systems might consider contrast and illumination conditions for becoming robust when applied to samples under different tissue preparations. [7] suggests that a proposed algorithm can consider the image quality as a parameter for its processing.

The high rate of false positive regions is still a challenge for lymphoma histological images segmentation. According to some studies from Table 1, analysis of more features is necessary to overcome this

limitation [8,46]. For instance, more topological and morphological features could be obtained through refinements in the MBIR, as suggested by [37]. Furthermore, semantics features could be investigated for lymphoma images segmentation, which these features represent criteria used by pathologists in histopathological image analysis for diagnoses [70].

The studies [22,35,53] and [54] showed that split touching nuclei or cytoplasmic regions is another problem in part of segmentation methods of lymphoma. The paper of [35] suggests to consider spatial connectivity, staining variations, curve fitting and geometrical features of the ROIs to overcome this problem.

The least used techniques for lymphoma images segmentation are based on edge detection. Comparison among the articles that used this methodology became complex due to the evaluation metrics used by each one of them. The histogram-based methods and classification techniques are the most used for segmentation of the considered lymphoma types. The Otsu method demands no user interaction, but it is susceptible to the image quality. Some studies, such as [46], used the empirical definition of threshold values, limiting their applications in real clinical environments. Considering classification techniques, training sets and a strategy to define optimum parameters can be necessary. [45] stresses the automatic estimation of inner parameters using, for instance, genetic algorithm [71], cuckoo search [72], artificial bee colony [73], differential evolution [74], particle swarm optimization [75] and wind driven optimization [76].

Therefore, various segmentation methods for regions of interest identification of lymphoma histological images are proposed in the literature. However, new or extensions of computational methods (pre-processing, detection/segmentation and post-processing) of different types of histological samples (CLL, FL and MCL) are issues which should be investigated to achieve clinically applicable results.

Acknowledgements

T.A.A.T. and M.Z.N. thank to CAPES (1575210) and FAPEMIG (TEC - APQ-02885-15) for financial support.

References

- [1] incidência de câncer no brasil; 2016 Instituto Nacional de Câncer José Alencar Gomes da Silva e Ministério da Saúde. Estimativa; 2016. URL, goo.gl/0dJfKk [Accessed 17 February 2017].
- [2] Orlov NV, Chen WW, Eckley DM, Macura TJ, Shamir L, Jaffe ES, et al. Automatic classification of lymphoma images with transform-based global features. *IEEE Trans Inf Technol Biomed* 2010;14(4):1003–13.
- [3] Mauriño BB, Siqueira SAC. In: Martins MA, Carrilho FJ, Alves VAF, Castilho EA, Cerri GG, Wen CL, editors. *Classificação dos linfomas*. São Paulo: Manole: Clínica Médica; 2011. p. 174–88.
- [4] Santos FPS, Fernandes GS. Linfomas não-Hodgkin. *MedicinaNet*; 2008. URL, goo.gl/YPIbCP [Accessed 17 February 2017].
- [5] Canellos GP, Lister TA, Young B. *The lymphomas*. second ed. London: Saunders; 2006.
- [6] Sertel O, Lozanski G, Shanaah A, Gurcan MN. Computer-aided detection of centroblasts for follicular lymphoma grading using adaptive likelihood-based cell segmentation. *IEEE Trans Biomed Eng* 2010;57(10):2613–6.
- [7] Belkacem-Boussaid K, Samsi S, Lozanski G, Gurcan MN. Automatic detection of follicular regions in h&e images using iterative shape index. *Comput Med Imaging Graph* 2011;35(7):592–602.
- [8] Sertel O, Catalyurek UV, Lozanski G, Shanaah A, Gurcan MN. An image analysis approach for detecting malignant cells in digitized h&e-stained histology images of follicular lymphoma. In: 20th IEEE international conference on pattern recognition; 2010. p. 273–6.
- [9] Gurcan MN, Boucheron L, Can A, Madabhushi A, Rajpoot N, Yener B. Histopathological image analysis: a review. *IEEE Rev Biomed Eng* 2009;2:147–71.
- [10] He L, Long LR, Antani S, Thoma GR. Histology image analysis for carcinoma detection and grading. *Comput Methods Programs Biomed* 2012;107(3):538–56.
- [11] Haggerty JM, Wang XN, Dickinson A, O'Malley CJ, Martin EB. Segmentation of epidermal tissue with histopathological damage in images of haematoxylin and eosin stained human skin. *BMC Med Imaging* 2014;14(1).
- [12] Ong SH, Jin CX, Jayasooriah Sinniah R. Image analysis of tissue sections. *Comput Biol Med* 1996;26(3):269–79.
- [13] do Nascimento MZ, Martins AS, Neves LA, Ramos RP, Flores EL, Carrijo GA. Classification of masses in mammographic image using wavelet domain features and polynomial classifier. *Expert Syst Appl* 2013;40(15):6213–21.
- [14] Irshad H, Veillard A, Roux L, Racoceanu D. Methods for nuclei detection, segmentation, and classification in digital histopathology: a review - current status and future potential. *IEEE Rev Biomed Eng* 2014;7:97–114.
- [15] Aswathy MA, Jagannath M. Detection of breast cancer on digital histopathology images: present status and future possibilities. *Informatics in Medicine Unlocked*. 2016.
- [16] Gartner LP, Hiatt JL. *Tratado de Histologia em Cores*. second ed. Rio de Janeiro: Guanabara Koogan; 2003.
- [17] Junqueira JC, Carneiro J. *Histologia básica*. tenth ed. Rio de Janeiro: Guanabara Koogan; 2004.
- [18] Guerdar EJ, Bishop MR. Overview of non-hodgkin's lymphoma. *Dis Mon* 2012; 58(4):208–18.
- [19] Oztan B, Kong H, Gurcan MN, Yener B. Follicular lymphoma grading using cell-graphs and multi-scale feature analysis. In: *SPIE medical imaging, international society for optics and photonics*; 2012. 8315:831516-1–; 831516-9.
- [20] Sertel O, Kong J, Lozanski G, Shana'ah A, Catalyurek U, Saltz J, et al. Texture classification using nonlinear color quantization: application to histopathological image analysis. In: *IEEE international conference on acoustics, speech and signal processing*; 2008. p. 597–600.
- [21] Buccheri V, Mauriño BB. In: Martins MA, Carrilho FJ, Alves VAF, Castilho EA, Cerri GG, Wen CL, editors. *Leucemia linfóide crônica*. São Paulo: Manole: Clínica Médica; 2011. p. 165–73.
- [22] Hallek M, Cheson BD, Catovsky D, Caligaris-Cappio F, Dighiero G, Döhner H, et al. Guidelines for the diagnosis and treatment of chronic lymphocytic leukemia: a report from the international workshop on chronic lymphocytic leukemia updating the national cancer institute-working group 1996 guidelines. *Blood* 2008;111(12): 5446–56.
- [23] Shamir L, Orlov N, Eckley DM, Macura TJ, Goldberg II IG, CBU. A proposed benchmark suite for biological image analysis. *Med Biol Eng Comput* 2008 2008; 46(9):943–7.
- [24] Dreyling M, Ghielmini M, Rule S, Salles G, Vitolo U, Ladetto M. Newly diagnosed and relapsed follicular lymphoma: esmo clinical practice guidelines for diagnosis, treatment and follow-up. *Ann Oncol* 2016;27(suppl 5):v83–90.
- [25] Dreyling M, Geisler C, Hermine O, Kluin-Nelemans HC, Goill SL, Rule S, et al. Newly diagnosed and relapsed mantle cell lymphoma: esmo clinical practice guidelines for diagnosis, treatment and follow-up. *Ann Oncol* 2014;25(Suppl 3): 83–9.
- [26] Cormack DH, Ham AW. A preparação de tecidos patológicos. In: *Histologia*. Rio de Janeiro: Guanabara Koogan; 1983.
- [27] Michail E, Dimitropoulos K, Koletsis T, Kostopoulos I, Grammalidis N. Morphological and textural analysis of centroblasts in low-thickness sliced tissue biopsies of follicular lymphoma. In: *Annual international conference of the IEEE engineering in medicine and biology society*; 2014. p. 3374–7.
- [28] Belsare AD, Mushrif MM. Histopathological image analysis using image processing techniques: an overview. *Signal & Image Process* 2012;3(4).
- [29] Kärnsnäs A. Image analysis methods and tools for digital histopathology applications relevant to breast cancer diagnosis. Ph.D. thesis. *Acta Universitatis Upsaliensis*; 2014.
- [30] Veta M, Pluim JP, van Diest PJ, Viergever MA. Breast cancer histopathology image analysis: a review. *IEEE Trans Biomed Eng* 2014;61(5):1400–11.
- [31] Rocha R, Vassallo J, Soares F, Miller K, Gobbi H. Digital slides: present status of a tool for consultation, teaching, and quality control in pathology. *Pathology-Research Pract* 2009;205(11):735–41.
- [32] Belkacem-Boussaid K, Prescott J, Lozanski G, Gurcan MN. Segmentation of follicular regions on h&e slides using a matching filter and active contour model. In: *SPIE medical imaging, international society for optics and photonics*; 2010. 7624: 762436-1–; 762436-11.
- [33] Sertel O, Kong J, Lozanski G, Catalyurek U, Saltz JH, Gurcan MN. Computerized microscopic image analysis of follicular lymphoma. In: *Medical imaging, international society for optics and photonics*; 2008. 6915:691535-1–; 691535-11.
- [34] Sertel O, Kong J, Catalyurek UV, Lozanski G, Saltz JH, Gurcan MN. Histopathological image analysis using model-based intermediate representations and color texture: follicular lymphoma grading. *J Signal Process Syst* 2009;55(1–3): 169–83.
- [35] Wootton R, Springall D, Polak J. *Image analysis in histology: conventional and confocal microscopy*. first ed. New York: Cambridge University Press; 1994.
- [36] Doyle S, Madabhushi A, Feldman M, Tomaszewski J. A boosting cascade for automated detection of prostate cancer from digitized histology. In: *International conference on medical image computing and computer-assisted intervention*; 2006. 4191:504–511.
- [37] do Nascimento MZ, Neves LA, Duarte SC, Duarte YAS, Batista VR. Classification of histological images based on the stationary wavelet transform. *J Phys Conf Ser* 2015:5741–4.
- [38] de Oliveira DLL, do Nascimento MZ, Neves LA, de Godoy MF, de Arruda PFF, de Neto DDS. Unsupervised segmentation method for cuboidal cell nuclei in histological prostate images based on minimum cross entropy. *Expert Syst Appl* 2013;40(18):7331–40.
- [39] Karaçalı B, Tözeren A. Automated detection of regions of interest for tissue microarray experiments: an image texture analysis. *BMC Med Imaging* 2007;7(1).
- [40] Yang L, Tuzel O, Meer P, Foran DJ. Automatic image analysis of histopathology specimens using concave vertex graph. *Med Image Comput Computer-Assisted Intervention* 2008;11:833–41.
- [41] Zorman M, Kokol P, Lenic M, de la Rosa JLS, Sigut JF, Alayon S. Symbol-based machine learning approach for supervised segmentation of follicular lymphoma images. In: *IEEE international symposium on computer-based medical systems*; 2007. p. 115–20.

- [45] Oger M, Belhomme P, Gurcan MN. A general framework for the segmentation of follicular lymphoma virtual slides. *Comput Med Imaging Graph* 2012;36(6): 442–51.
- [46] Michail E, Kornaropoulos EN, Dimitropoulos K, Grammalidis N, Koletsa T, Kostopoulos I. Detection of centroblasts in h&e stained images of follicular lymphoma. In: *Signal processing and communications applications conference*; 2014. p. 2319–22.
- [47] Gonzalez RC, Woods RE. *Processamento de imagens digitais*. first ed. São Paulo: Edgar Blücher; 1992.
- [48] Kandwal R, Kumar A, Bhargava S. Review: existing image segmentation techniques. *Int J Adv Res Comput Sci Softw Eng* 2014;4(4):153–6.
- [49] Luo Y, Celenk M, Bejai P. Discrimination of malignant lymphomas and leukemia using radon transform based-higher order spectra. In: *Medical imaging, international society for optics and photonics*; 2006. 6144:61445K-1 -61445K-10.
- [50] Kong H, Belkacem-Boussaid K, Gurcan M. Cell nuclei segmentation for histopathological image analysis. In: *SPIE medical imaging, international society for optics and photonics*; 2011. 7962:79622R-1 -79622R-14.
- [51] Kong H, Gurcan M, Belkacem-Boussaid K. Partitioning histopathological images: an integrated framework for supervised color-texture segmentation and cell splitting. *IEEE Trans Med Imaging* 2011;30(9):1661–77.
- [52] Arora B, Banerjee S. Computer assisted grading schema for follicular lymphoma based on level set formulation. In: *IEEE students conference on engineering and systems*; 2013. p. 1–6.
- [53] Mohammed EA, Mohamed MMA, Naugler C, Far BH. Chronic lymphocytic leukemia cell segmentation from microscopic blood images using watershed algorithm and optimal thresholding. In: *Annual IEEE canadian conference on electrical and computer engineering*; 2013. p. 1–5.
- [54] Mohammed EA, Far BH, Naugler C, Mohamed MMA. Application of support vector machine and k-means clustering algorithms for robust chronic lymphocytic leukemia color cell segmentation. In: *International Conference on e-Health Networking, Applications & Services*; 2013. p. 622–6.
- [55] Dimitropoulos K, Michail E, Koletsa T, Kostopoulos I, Grammalidis N. Using adaptive neuro-fuzzy inference systems for the detection of centroblasts in microscopic images of follicular lymphoma. *Signal, Image Video Process* 2014;8(1): 33–40.
- [56] Dimitropoulos K, Barmpoutis P, Koletsa T, Kostopoulos I, Grammalidis N. Automated detection and classification of nuclei in pax5 and h&e-stained tissue sections of follicular lymphoma. *Signal, Image Video Process* 2016;11(1):145–53.
- [57] Chan TF, Vese LA. Active contours without edges. *IEEE Trans Image Process* 2001; 10(2):266–77.
- [58] Li C, Kao C, Gore JC, Ding Z. Minimization of region-scalable fitting energy for image segmentation. *IEEE Trans Image Process* 2008;17(10):1940–9.
- [59] He L, Long R, Antani S, Thoma GR. Computer assisted diagnosis in histopathology. In: Zhao Z, editor. *Sequence and genome analysis: methods and applications*; 2010. p. 271–87.
- [60] Otsu N. A threshold selection method from gray-level histograms. *IEEE Trans Syst Man, Cybern* 1979;9(1):62–6.
- [61] Yang L, Meer P, Foran DJ. Unsupervised segmentation based on robust estimation and color active contour models. *IEEE Trans Inf Technol Biomed* 2005;9(3):475–86.
- [62] Chetverikov D, Szabo Z. A simple and efficient algorithm for detection of high curvature points in planar curves. *Workshop of the Austrian Pattern Recognition Group*. 1999. p. 175–84.
- [63] Janssens T, Antanas L, Derde S, Vanhorebeek I, Van den Bergh G, Grandas FG. Charisma: an integrated approach to automatic h&e-stained skeletal muscle cell segmentation using supervised learning and novel robust clump splitting. *Med Image Anal* 2013;17(8):1206–19.
- [64] Ghose S, Oliver A, Martí R, Lladó X, Vilanova JC, Freixenet J, et al. A survey of prostate segmentation methodologies in ultrasound, magnetic resonance and computed tomography images. *Comput Methods Programs Biomed* 2012;108(1): 262–87.
- [65] Byrd KA, Zeng J, Chouikha M. A validation model for segmentation algorithms of digital mammography images. *J Appl Sci Eng Technol* 2007;1:41–50.
- [66] Macenko M, Niethammer M, Marron JS, Borland D, Woosley JT, Guan X, et al. A method for normalizing histology slides for quantitative analysis. In: *International symposium on biomedical imaging: from nano to macro*; 2009. 9:1107–1110.
- [67] Vahadane A, Peng T, Albarqouni S, Baust M, Steiger K, Schlitter AM, et al. Structure-preserved color normalization for histological images. In: *IEEE international symposium on biomedical imaging*; 2015. p. 1012–5.
- [68] Vahadane A, Peng T, Sethi A, Albarqouni S, Wang L, Baust M, et al. Structure-preserving color normalization and sparse stain separation for histological images. *IEEE Trans Med Imaging* 2016;35(8):1962–71.
- [69] Li X, Plataniotis KN. A complete color normalization approach to histopathology images using color cues computed from saturation-weighted statistics. *IEEE Trans Biomed Eng* 2015;62(7):1862–73.
- [70] Mosquera-Lopez C, Agaian S, Velez-Hoyos A, Thompson I. Computer-aided prostate cancer diagnosis from digitized histopathology: a review on texture-based systems. *IEEE Rev Biomed Eng* 2015;8:98–113.
- [71] Ghosh P, Mitchell M, Tanyi JA, Hung AY. Incorporating priors for medical image segmentation using a genetic algorithm. *Neurocomputing* 2016;195:181–94.
- [72] Ilunga-Mbuyamba E, Cruz-Duarte JM, Avina-Cervantes JG, Correa-Cely CR, Lindner D, Chalopin C. Active contours driven by cuckoo search strategy for brain tumour images segmentation. *Expert Syst Appl* 2016;56:59–68.
- [73] Bose A, Mali K. Fuzzy-based artificial bee colony optimization for gray image segmentation. *Signal, Image Video Process* 2016;10(6):1089–96.
- [74] Cuevas E, Zaldívar D, Perez-Cisneros M. Image segmentation based on differential evolution optimization. In: *Applications of evolutionary computation in image processing and pattern recognition*; 2016. p. 9–22.
- [75] Remamany KP, Chelliah TR, Chandrasekaran K, Subramanian K. Brain tumor segmentation in mri images using integrated modified pso-fuzzy approach. *Int Arab J Inf Technol* 2015;12(6A):797–804.
- [76] Bayraktar Z, Komurcu M, Werner DH. Wind driven optimization (wdo): a novel nature-inspired optimization algorithm and its application to electromagnetics. In: *IEEE antennas and propagation society international symposium*; 2010. p. 1–4.